

IRRADIATION EFFECTS ON THE SURFACE REACTIONS OF METALS

Summary Report October 1, 1958, to November 1, 1959

By
F. D. Carpenter
J. L. White

December 15, 1959

General Dynamics Corporation
General Atomic Division
San Diego, California



DISCLAIMER

Portions of this document may be illegible in electronic image products. Images are produced from the best available original document.

LEGAL NOTICE

This report was prepared as an account of Government sponsored work. Neither the United States, nor the Commission, nor any person acting on behalf of the Commission:

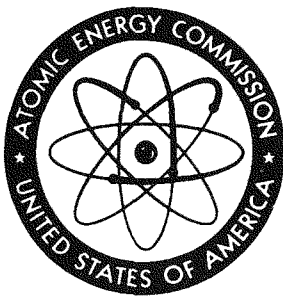
A. Makes any warranty or representation, expressed or implied, with respect to the accuracy, completeness, or usefulness of the information contained in this report, or that the use of any information, apparatus, method, or process disclosed in this report may not infringe privately owned rights; or

B. Assumes any liabilities with respect to the use of, or for damages resulting from the use of any information, apparatus, method, or process disclosed in this report.

As used in the above, "person acting on behalf of the Commission" includes any employee or contractor of the Commission, or employee of such contractor, to the extent that such employee or contractor of the Commission, or employee of such contractor prepares, disseminates, or provides access to, any information pursuant to his employment or contract with the Commission, or his employment with such contractor.

This report has been reproduced directly from the best available copy.

Printed in USA. Price \$1.00. Available from the Office of Technical Services, Department of Commerce, Washington 25, D. C.



GA-1093

IRRADIATION EFFECTS ON THE SURFACE
REACTIONS OF METALS

Summary Report

October 1, 1958, to November 1, 1959

Contract AT(04-3)-179

Work done by:

J. L. White
M. T. Simnad
F. D. Carpenter
W. L. Kosiba
D. W. Blethrow
R. C. Weed
C. C. Morris

Report written by:

F. D. Carpenter
J. L. White

Project No. 37

December 15, 1959

GENERAL ATOMIC

DIVISION OF GENERAL DYNAMICS CORPORATION

•
JOHN JAY HOPKINS LABORATORY
FOR PURE AND APPLIED SCIENCE

SAN DIEGO 12, CALIFORNIA

I. INTRODUCTION

The continuing purpose of this research program is to develop an experimental basis for a fundamental understanding of the effects of radiation on the surface reactions of metals and metal oxides. Since the issuance of the last summary report, ^{(1)*} considerable progress has been made in the development of facilities for studying the processes of oxidation, reduction, and dissolution of irradiated specimens; representative experimental results are reported in Sections II and III. These results have shown several interesting effects of reactor radiation, particularly with respect to the enhanced chemical reactivity of irradiated crystals. A facility for the study of oxidation and reduction kinetics within the radiation fields of a reactor core has also been completed and is described in Section II.

The surface reactions of a crystal with a gas or liquid phase may be influenced by radiation in two ways: by activation of the reactant species in the gaseous or liquid environment, or by alteration of the structure of the crystal surface. ⁽²⁾ It is desirable to investigate these effects separately as far as possible, and most of the work to date has concerned the reactivity of metals and metal oxides previously subjected to reactor radiation. Thus, from a general viewpoint, attention has been focused on the nature of a radiation-induced crystal defect under such conditions that it is no longer within the bulk of the crystal but rather at or near the surface, where it may either impart enhanced reactivity to the crystal itself or act as a catalytic site for another reaction.

II. REACTIONS WITH GAS PHASES

The experimental facilities for the study of the reactions of metals and metal oxides with gas phases have been extended as follows: (1) the

*References are listed on page 38.

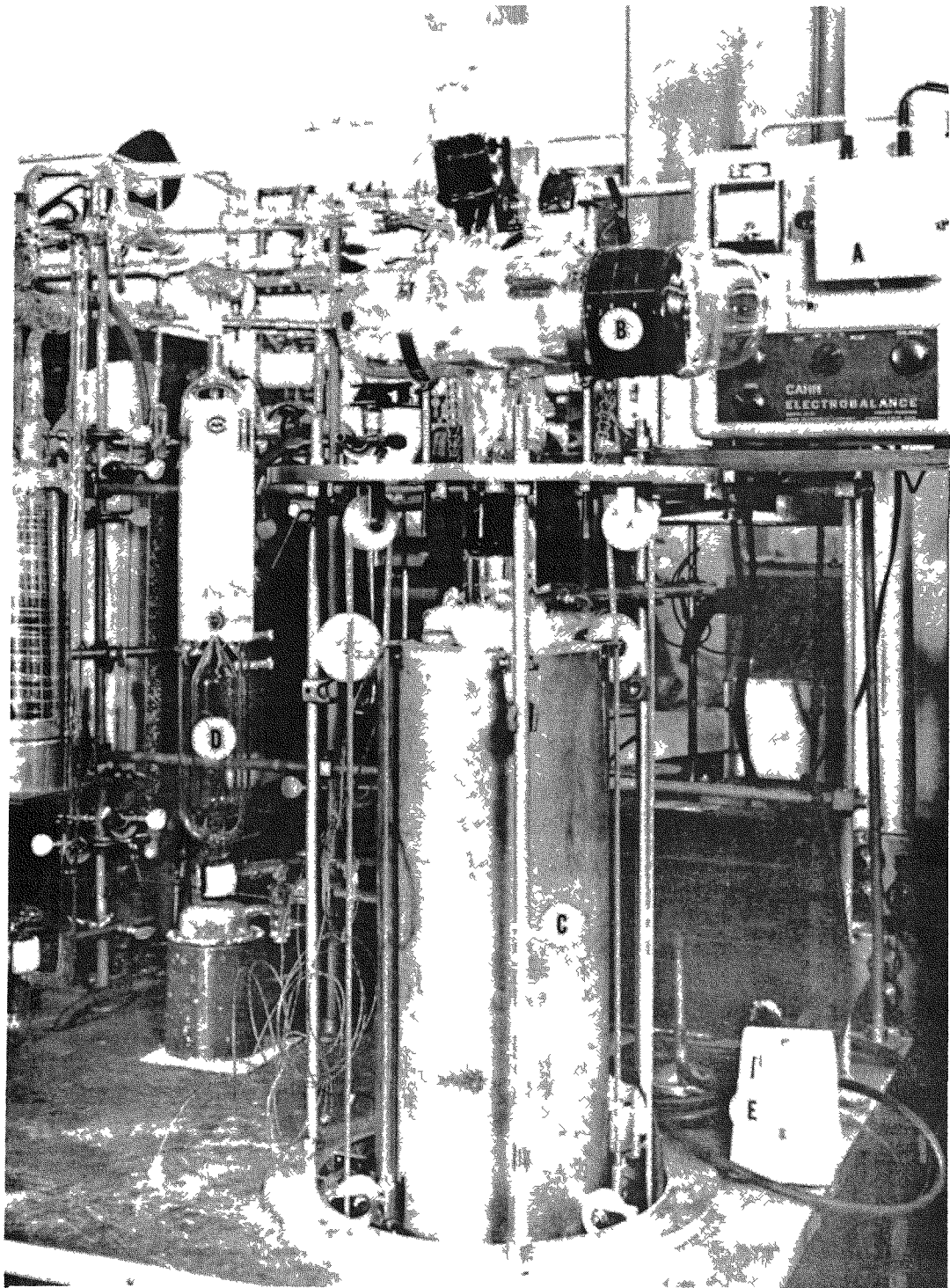
existing microbalance system has been modified for greater stability; (2) an automatic recording microbalance has been built which provides increased sensitivity for investigations in the region of thin films of oxide; and (3) a watertight furnace assembly for insertion into the core of the TRIGA reactor⁽³⁾ has been developed for the study of reactions in the radiation field of the reactor. The oxidation of copper and the subsequent reduction of copper oxide were selected for the initial investigations, as extensive information is available on the oxidation of copper outside of radiation fields.⁽⁴⁻⁹⁾ Furthermore, copper of high purity does not develop a high level of radioactivity on irradiation and may thus be studied without excessive experimental difficulties.

REACTIONS OF COPPER AND COPPER OXIDE

For studies of the oxidation and reduction of copper and copper oxide, modifications have been made in the microbalance system previously described⁽¹⁾ in order to attain improved stability for long-term experiments, more uniform temperatures, greater load capacity, and more convenience in routine operation. A general view of the present system is shown in Fig. 1.

The thermal environment for the reactions has been improved by the use of a Nichrome-wound furnace with six taps to permit precise adjustment of power in various parts of the furnace. An aluminum block 3 in. in diameter and 9 in. in length, placed within the furnace core and drilled to take the silica reaction tube, provides additional thermal stability and uniformity and also acts as a grounded shield.

The control system for the Cahn electromagnetic microbalance has been modified by the use of constant-voltage, direct-current power supplies instead of the original batteries. This has effectively eliminated the balance calibration drift in long-term experiments. The sensitivity, reproducibility, and linearity of the microbalance system have been found to be within $\pm 1 \mu\text{g}$, and the maximum balance load has been increased to 40 mg by modifying the



- Ⓐ Microbalance control system Ⓓ Vacuum gauge
Ⓑ Microbalance housing Ⓔ Timer
Ⓒ Furnace suspended on counterweighted pulley system

Fig. 1--General view of microbalance system

balance beam. The electrostatic effects commonly associated with such microbalances have been effectively counteracted by the use of a fine Nichrome suspension wire through which the specimen may be grounded whenever necessary.

The major portions of the oxidation and reduction of copper have been made at 150°C , well below the temperature (350°C) at which the radiation hardening of copper has been found to anneal.⁽¹⁰⁾ The oxidation reactions were carried out at a pressure of 10 mm Hg of purified oxygen. These conditions were selected on the basis of preliminary studies performed to learn (1) the characteristics of the balance, e. g., the effects of buoyancy and convection, and (2) the minimum temperature at which a reproducible and conveniently measurable rate of oxidation could be obtained.

The copper specimens were prepared by rolling copper of high purity to a thickness of 0.001 in. Several intermediate anneals at 750°C were performed during the reduction process, and the specimens were rolled in sandwiches between sheets of pure copper to avoid the introduction of impurities. The specimens had a nominal area of 2 to 4 cm^2 . The foils were given a final anneal at 900°C for 24 hr in vacuum. The foils were cleaned by dipping them in 10% HNO_3 and then rinsing them in distilled water, acetone, and 1% H_3PO_4 . A reproducible surface was then prepared by electropolishing them in 70% H_3PO_4 . The residual phosphate films were removed by successive rinses of 1% H_3PO_4 , dilute HNO_3 , distilled water, and acetone, and the foils were then stored under dry acetone until they were mounted on the microbalance suspension.

Before a specimen was mounted on the balance suspension, the gas purification system was flushed thoroughly and the microbalance system was degassed. Pure argon was introduced into the microbalance system at a pressure about 30 mm Hg above atmospheric pressure. The microbalance system was then opened, and the specimen was transferred from the suspension. The system was then closed and pumped down to a pressure of 10^{-5} mm Hg. The furnace was raised into position, and stable weight

readings and uniformity of temperature were achieved before the reactant gas was admitted.

An oxidation curve representative of the results obtained in the initial studies of annealed copper is shown in Fig. 2. A parabolic oxidation-rate relationship has been fitted to the data, i. e.,

$$\Delta m = 0.105 \sqrt{t},$$

where Δm is the weight gain in micrograms and t is the time in seconds. It was observed in a number of runs that this relationship was only approximately valid for the relatively thin oxide films (of the order of 2000 Å); this agrees with the observations of earlier workers,^(5,6) who found that the initial oxidation of copper cannot be represented by a simple analytical relation.

In order to understand further the chemical nature of the metal surfaces prepared by treatments with hydrogen, the rates of oxidation of copper specimens previously subjected to oxidation and reduction were investigated, and one set of results is shown in Fig. 3. Only the first oxidation yields results which are characteristic of the surface as originally prepared; subsequent oxidations show a rapid rate of reaction in the initial period, followed by a rate curve parallel to the later stage of the first oxidation. The results indicate that the copper resulting from the reduction of the film of Cu_2O is deposited in a state of enhanced reactivity on the surface of the original copper specimen. Thus, cleaning processes employing hydrogen reduction to remove oxide films of appreciable thickness may lead to initial oxidation rates which are not typical of the bulk crystal.

In the earlier studies described in the first summary report (see Ref. 1), the cold-working of copper was shown to have an appreciable effect on the rate of oxidation, particularly in the thin-film region up to a weight increase of about $5 \mu\text{g cm}^{-2}$. These results were in agreement with the observations of Lustman and Mehl,⁽⁶⁾ and on the basis of these investigations an annealing temperature of 900°C was selected to ensure complete annealing of the cold work.

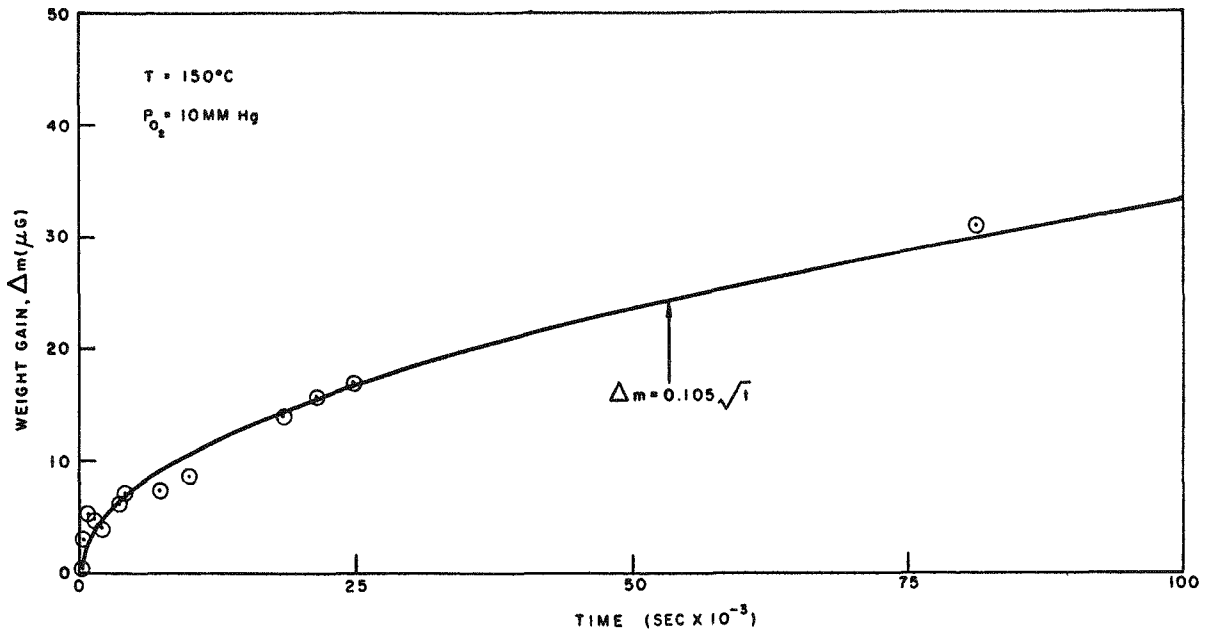


Fig. 2--Oxidation of copper foil annealed at 900°C
 (surface area of specimen, 2.53 cm^2)

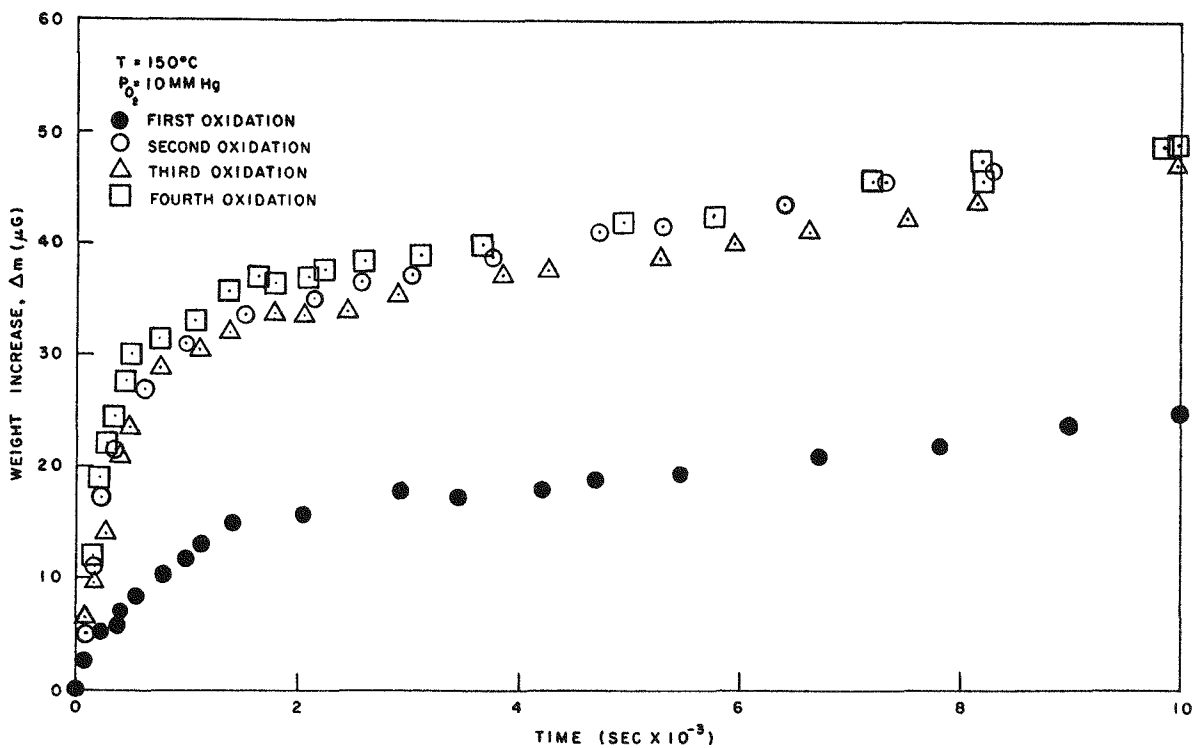


Fig. 3--Effect of previous oxidations and reductions on the rate of oxidation of pure copper; the Cu_2O films were reduced at 150°C with H_2 at 1 atm pressure

The measured weight increases during the oxidation of irradiated foils of pure copper are compared with the measurements on unirradiated foils in Fig. 4. Every effort was made to give the two sets of foils identical preparation; the set of control specimens was stored in sealed glass capsules under vacuum for a period similar to that required for the irradiation, in similar capsules, of the second set. The second set of specimens was irradiated in the Brookhaven National Laboratory reactor, where they received a total integrated flux of $nvt = 2.5 \times 10^{19}$ neutrons cm^{-2} .

Despite some scatter in the data of Fig. 4, the irradiated specimens showed greater weight increases than did the unirradiated specimens in the same time intervals. The enhanced reactivity appears to be strongest in the thin-film region up to about $5 \mu\text{g cm}^{-2}$. Thus, the nucleation and growth of the thin film of oxide is markedly enhanced, but at film thicknesses above about 700 \AA the further growth of the oxide film is independent of the condition of the substrate metal.

In studies of copper where single crystals oxidized at 150°C during exposure to the radiation field of a reactor, Young⁽¹¹⁾ found evidence for enhanced oxidation rates in the thin-film region (of the order of 250 \AA). The present results, obtained on specimens oxidized after exposure to reactor radiation, indicate that the enhanced reactivity may be attributed to crystal defect structures, since they appear at a surface moving into the crystal body, rather than to activation of the gaseous reactants. That these effects apparently persist to oxide thicknesses corresponding to several hundred atom layers is not unexpected; studies of the rates of oxidation of various faces of single crystals of copper show similar substrate effects persisting to oxide film thicknesses as large as 1000 \AA .⁽⁷⁾ Furthermore, observations by electron microscopy of the films formed on different crystal faces show that the film structure is dependent on the surface of the metal crystal.⁽⁸⁾

X-ray diffraction patterns were obtained on several oxidized copper specimens, including both irradiated and unirradiated specimens. In each

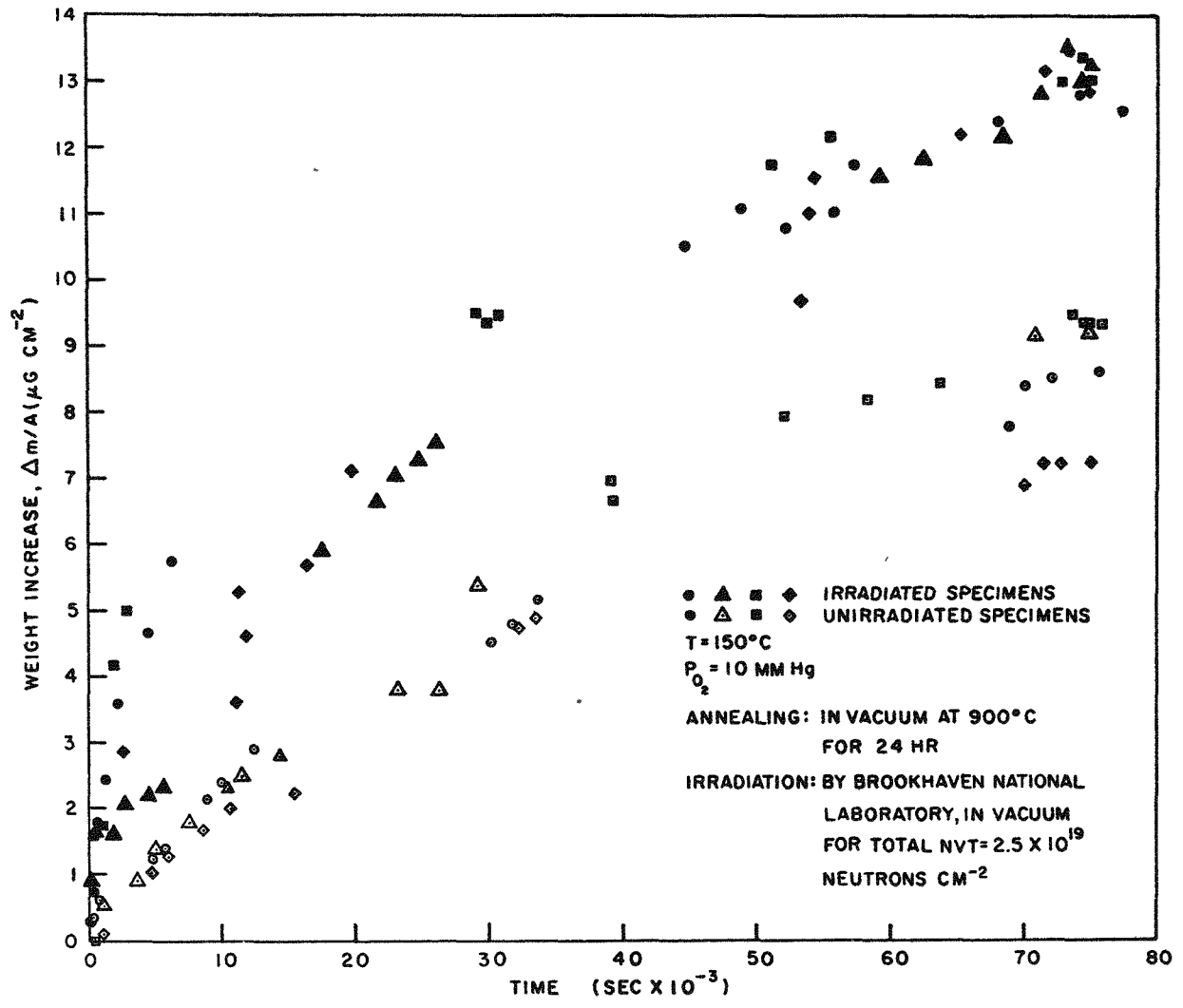


Fig. 4--Oxidation of irradiated and unirradiated copper foils

case the oxide thickness was of the order of 1200 Å. The oxide film was identified as Cu_2O and was shown to be stable after exposure to radiation. No CuO was detectable, indicating that the film contained less than 1% CuO , if any. Assuming that the films are entirely Cu_2O , the weight increases may be converted to average oxide film thicknesses by the relation

$$\frac{\Delta l}{\Delta m} = \frac{150}{A} ,$$

where Δl is the average film thickness in angstrom units, Δm is the weight increase in micrograms, and A is the surface area in square centimeters.

Several experiments have been made to determine the effect of radiation on the reduction of Cu_2O . For this purpose, annealed copper foils were oxidized at 250°C in O_2 at 1 atm for 20 min, which produced a film thickness of approximately 2500 Å. One set of foils was then irradiated in General Atomic's TRIGA reactor to a total irradiation of $nvt = 1.7 \times 10^{18}$ neutrons cm^{-2} and the second set was stored in the laboratory under similar ambient conditions. The specimens were then reduced in the microbalance system with H_2 gas at a pressure of 1 atm. The results of this experiment (see Fig. 5) indicate that the induction period, during which the reduction proceeds very slowly or not at all, is unaffected by radiation. In later stages of the reduction process, the reduction rates show a serious and as yet unexplained lack of reproducibility, and the effect of preirradiation of the oxide specimen appears to be less than the spread between results of independent runs on unirradiated specimens. In no case were the specimens fully reduced. Further experiments are planned to investigate the reduction phenomena more fully.

In another set of experiments, to investigate the effect of radiation on the properties of a thin film of Cu_2O on a pure copper substrate, two sets of copper-foil specimens were first oxidized to a film thickness of about 1300 Å by exposure to O_2 gas at 150°C and 10 mm Hg for a period of 75,000 sec. Separate oxidations were performed in the Cahn microbalance system

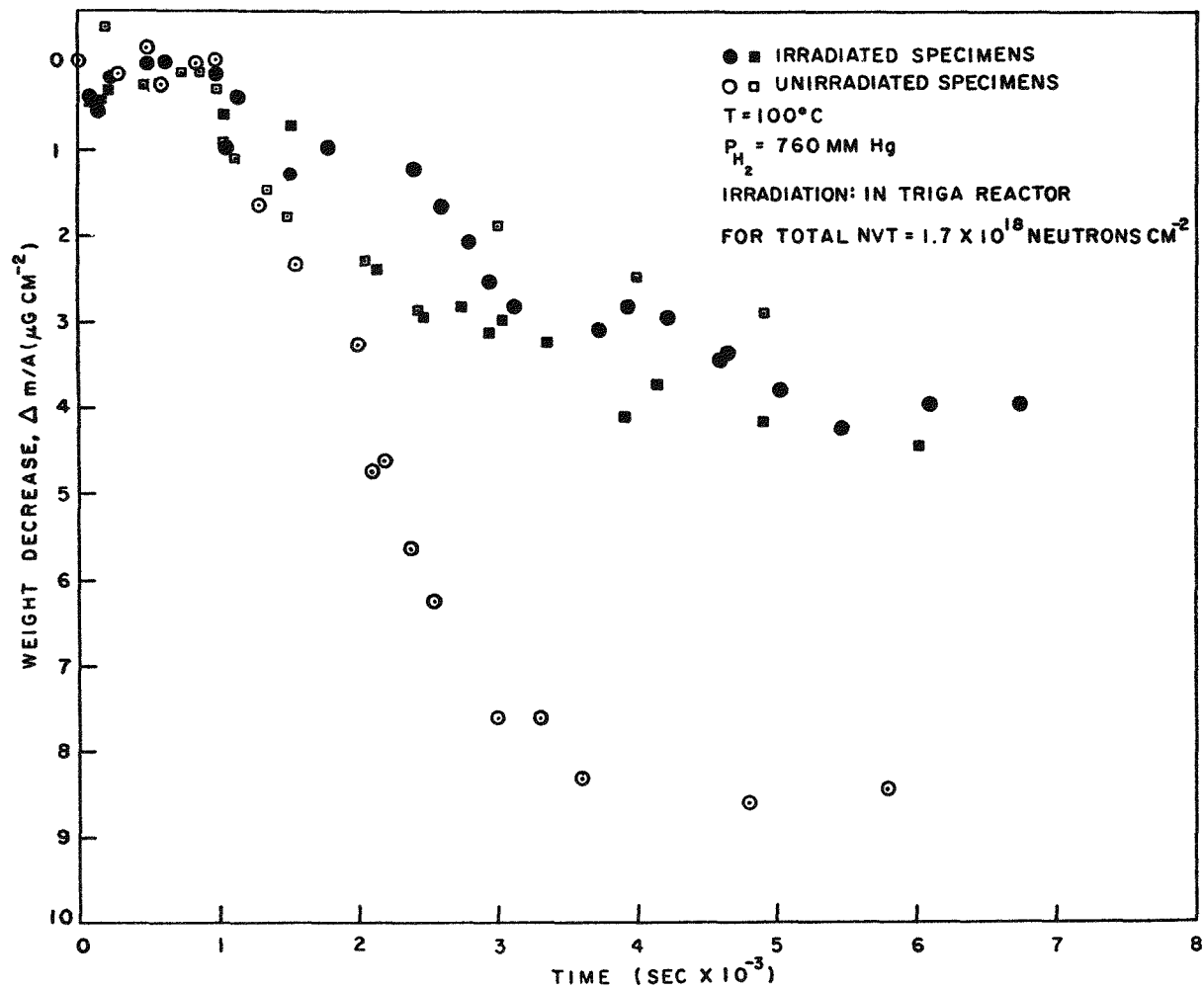


Fig. 5--Reduction of irradiated and unirradiated films of Cu₂O formed by prior oxidation of the copper substrate

for each specimen in order to establish the characteristic primary oxidation curves for each specimen. Each set of specimens was then sealed under vacuum into a vitreous silica capsule. One capsule was irradiated in the TRIGA reactor and received a total irradiation of $nvt = 3.4 \times 10^{18}$ neutrons cm^{-2} , and the second capsule was stored under similar ambient conditions. After completion of the irradiation, each specimen was further oxidized in the Cahn microbalance system to determine changes in the oxidation kinetics. Each experiment was concluded by reduction of the specimens in H_2 gas at 1 atm and 150°C .

The results of two experiments on the $\text{Cu}/\text{Cu}_2\text{O}$ specimens are given in Fig. 6. Since the Cahn microbalance measures only weight changes and does not have sufficient capacity in the present application to weigh the entire specimen, the data have been plotted on the assumption that the weight in vacuum at the start of the primary oxidation is equal to the weight in vacuum at the conclusion of the reduction process.

In three out of four cases the unirradiated specimens exhibited the behavior shown in Fig. 6; i. e., the secondary oxidation proceeded in an apparently uninterrupted fashion, with only a slight mismatch at the point of interruption of the oxidation process. On the other hand, all the $\text{Cu}/\text{Cu}_2\text{O}$ specimens that were removed for irradiation displayed a large gap at the point of interruption for irradiation, and the kinetics of the secondary oxidation were markedly decreased. For both the irradiated and unirradiated specimens, the reduction with H_2 proceeded smoothly and rapidly. The data for the reduction process are plotted on a scale amplified by a factor of four.

The implications of the data given in Fig. 6 are believed to be of importance to the general field of radiation effects with respect to the technique of irradiation. A plausible explanation of the interrupted oxidation curve for the irradiated specimen is that even though the irradiation was conducted at an ambient reactor temperature of about 25°C and the capsules were originally sealed under vacuum, the specimen suffered either further oxidation or the transfer of mass from the capsule to its surface to the

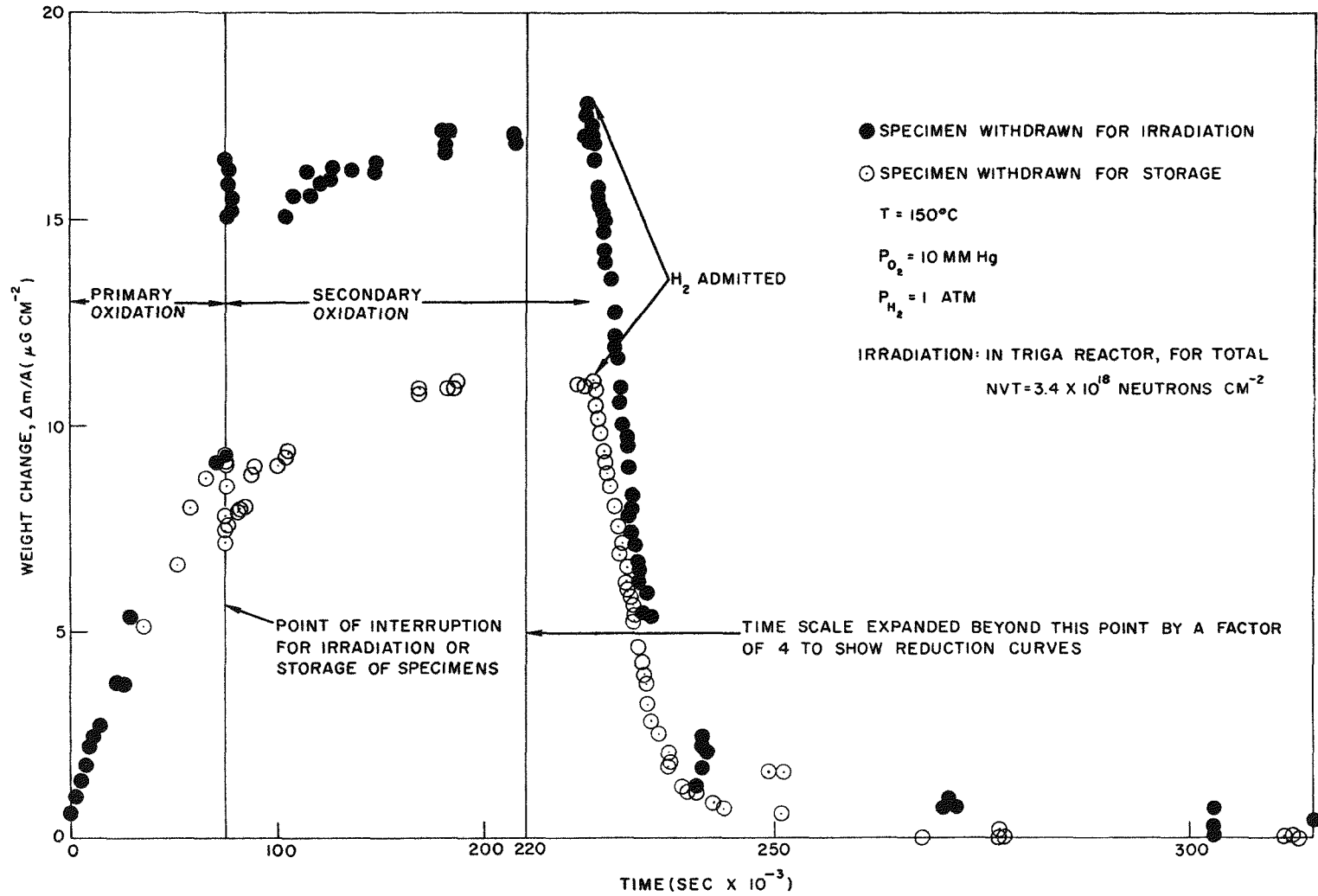


Fig. 6--Oxidation and subsequent reduction of Cu/Cu₂O specimens

extent of about $6 \mu\text{g cm}^{-2}$. The large decrease in weight during the reduction process implies that the mechanism of weight increase during irradiation involved either oxidation or the transfer of a readily reducible oxide to the surface of the $\text{Cu/Cu}_2\text{O}$ specimen. Further experiments are planned to investigate these phenomena more fully.

DEVELOPMENT OF AN AUTOMATIC RECORDING MICROBALANCE OF HIGH SENSITIVITY

The results of the investigations reported in the previous section emphasize the importance of studies of reactions in the thin-film region, where irradiation of the crystal phase has been shown to have a marked influence on the kinetics of the surface reactions. Although improvements in the present microbalance facilities have resulted in a sensitivity of $\pm 0.2 \mu\text{g cm}^{-2}$ for copper specimens, this corresponds to a sensitivity to thickness of only $\pm 75 \text{ \AA}$. In order to extend the investigations to a sensitivity of the order of $\pm 0.01 \mu\text{g cm}^{-2}$ (corresponding to a hypothetical thickness sensitivity of $\pm 1.5 \text{ \AA}$ for Cu_2O), a microbalance intended to achieve a sensitivity of $\pm 0.1 \mu\text{g}$ and a maximum load of 750 mg is being developed. For greater convenience in the experimental work, and with a view toward making measurements possible in radiation fields of such intensity as to create a health hazard in the vicinity of the apparatus, this microbalance is being developed as an automatic recording device capable of remote operation when desired.

The design of the microbalance follows that of conventional torsion-fiber microbalances made of vitreous silica; such microbalances, which are thoroughly described in the literature,⁽¹²⁻¹⁴⁾ can reach sensitivities in excess of that necessary for the investigations planned. The principal objective in the development of the present apparatus is to couple the torsion-fiber microbalance to an automatic recording system without excessive loss of sensitivity and with maximum flexibility with respect to sample size,

material, and radiation field. The sensing device selected for the beam displacements, is a variable-permeance transducer; a similar technique has been employed by Cochran⁽¹⁵⁾ in developing a null-balance automatic recorder for a microbalance of the type designed by Czanderna and Honig.⁽¹⁶⁾

The microbalance and vacuum system are shown schematically in Fig. 7. General views of the apparatus in its present state of development are shown in Fig. 8, and Fig. 9 is a more detailed view of the microbalance in its vacuum housing. The automatic recording microbalance system comprises four major components: (1) the microbalance and the sensing element for the beam position, (2) the vacuum and gas-purification system, (3) the servo-control system, and (4) the recorder, which produces a continuous graphic record of the weight change as a function of time.

The frame and beam of the microbalance are constructed from vitreous silica rod 2 mm in diameter. The beam is suspended in the center of the frame by a tungsten torsion fiber 0.001 in. in diameter. The fiber is cemented in position with silver chloride. The left arm of the beam supports the transducer sensing probe and a compensating solenoid, and the right arm supports the specimen hanging in the furnace.

The electrical circuit for the control and recording system is illustrated in Fig. 10. The compensating solenoid consists of a tare coil and a nulling coil, which act on a Cunife magnet suspended below the variable-permeance transducer probe. The tare coil, which is not a part of the automatic recording circuit, serves to bring the balance to null at the outset of an experiment. The nulling coil is actuated by the control system to correct for the nonlinearity of the output signal from the sensing transducer. This nonlinearity relative to the probe displacement results from the movement of the Cunife magnet in the field of the tare coil.

Several calibration experiments have been done on the complete system with satisfactory results as to the performance of the control and recording systems. However, the sensitivity of the system requires that more elaborate mechanical damping and a constant-temperature environment

TO GAS - PURIFICATION TRAIN

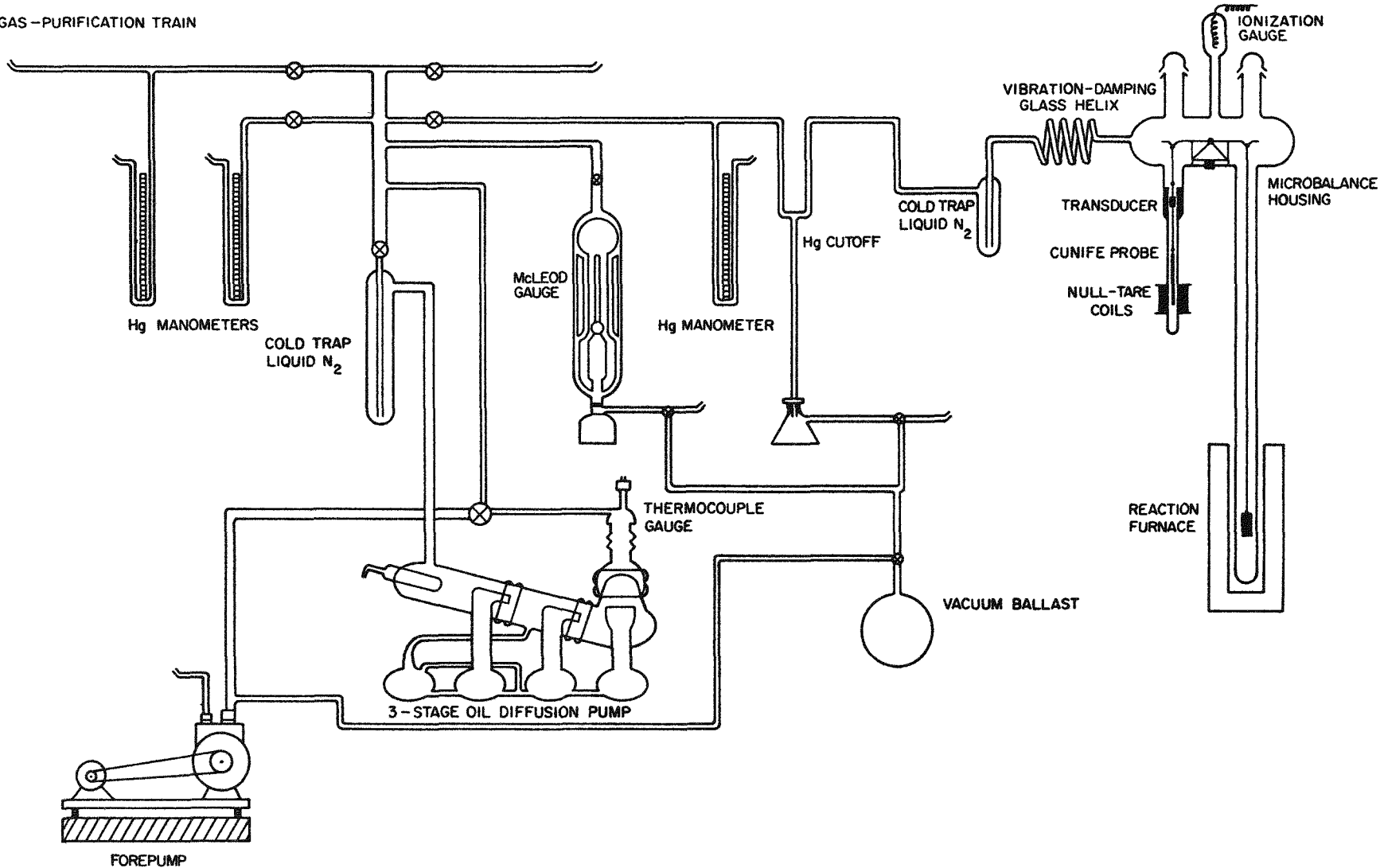


Fig. 7--Torsion-fiber microbalance system as designed for operation as an automatic recording microbalance

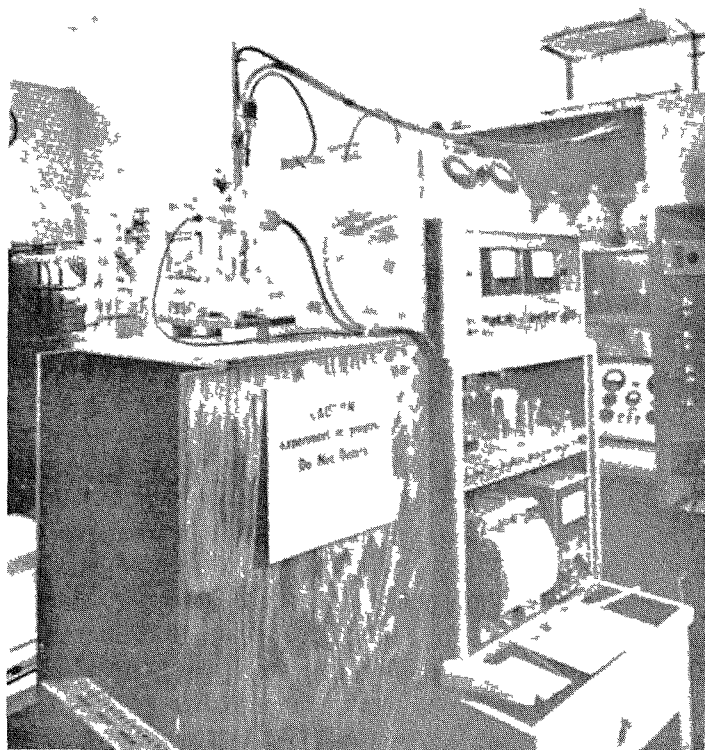
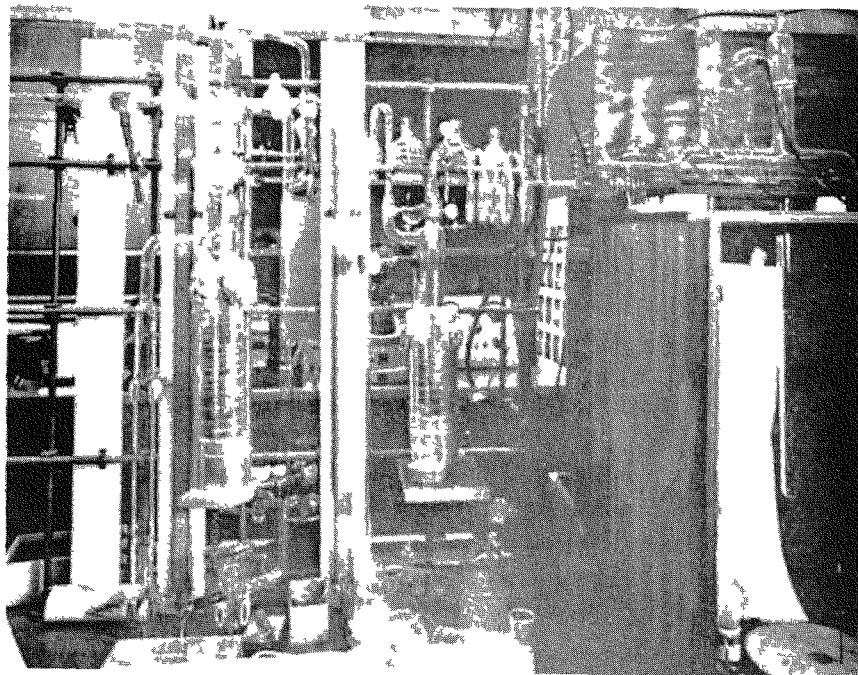


Fig. 8--The automatic recording microbalance; (top) front view showing relation of vacuum system to microbalance and furnace, (bottom) side view showing recording and control system for microbalance

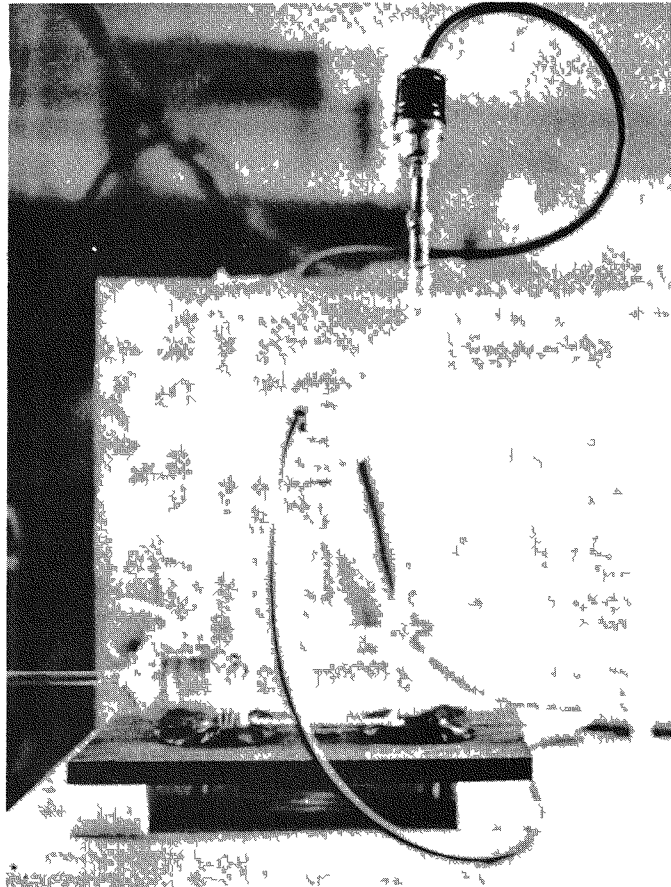


Fig. 9--Microbalance and housing, with balance in position for calibration tests

be provided for the microbalance system before further tests are undertaken.

DEVELOPMENT OF FURNACE FOR STUDIES IN REACTOR RADIATION FIELDS

The effect of reactor radiation in activating the gaseous reactants will be studied by measuring the rates of reaction of metals and metal oxides with gases during exposure to a radiation field. For this purpose, a furnace has been designed and constructed for operation within the General Atomic TRIGA reactor.⁽³⁾ The out-of-reactor tests on the furnace have been completed successfully, and the furnace and connecting tubes are being

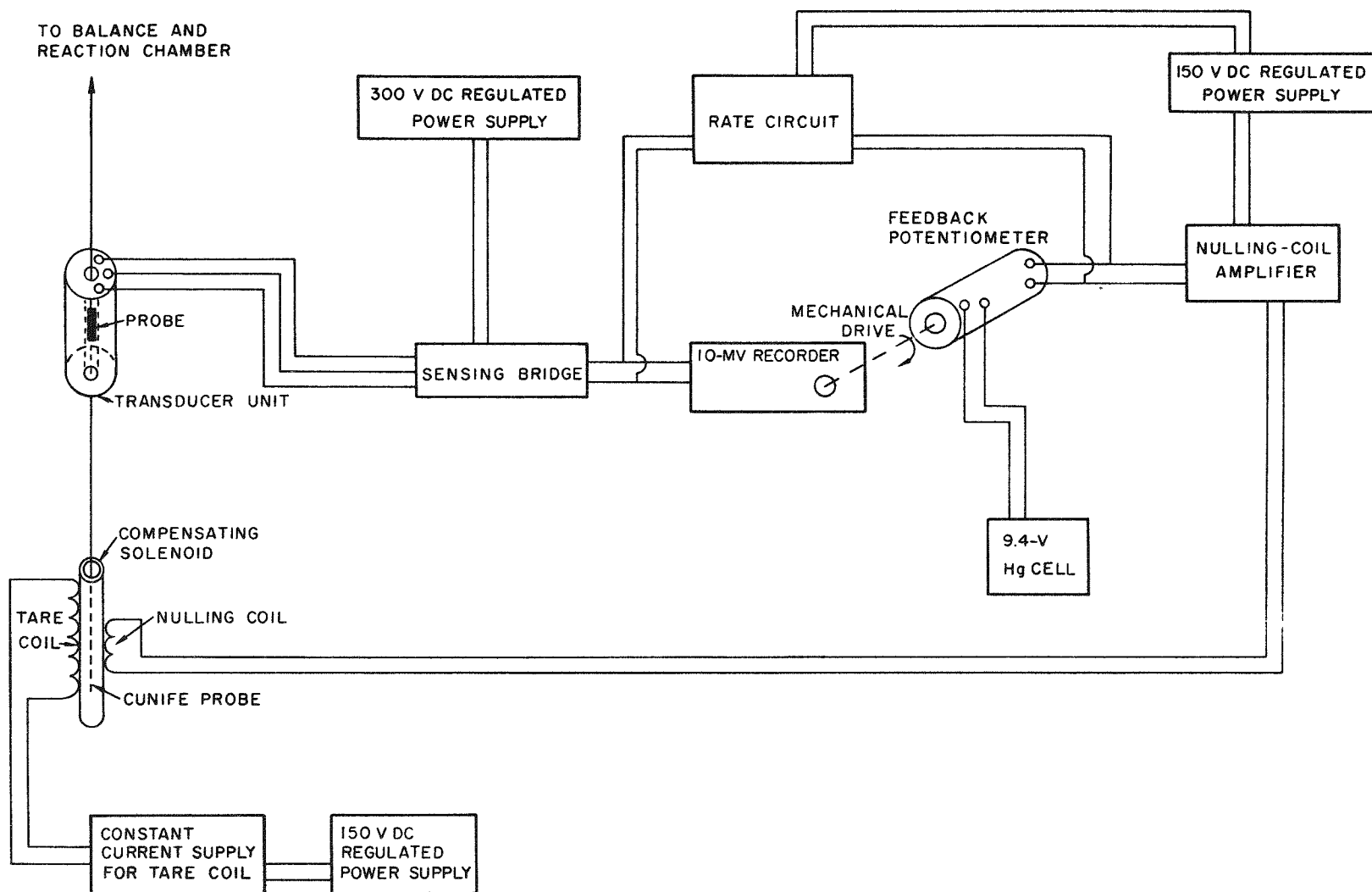


Fig. 10--Electronic components of automatic recording microbalance

prepared for insertion into a position immediately adjacent to the core of the reactor (see Fig. 11).

The design of the TRIGA reaction furnace is shown in Fig. 12. Figure 13 is a view of the furnace disassembled to show the component parts. Materials of low cross section have been used insofar as possible to minimize perturbation of the reactor and to reduce the problem of disposal of the burned-out furnace. The internal parts of the furnace, including thermocouples and Al_2O_3 insulation, fit within a watertight fuel-element can, which is inserted into the reactor core. The Nichrome resistor wire is insulated by ceramic "fish spines" and is wound on a 7/8-in. -OD aluminum furnace tube, which serves as one power lead. The furnace is fitted with thermocouples made of No. 24 gauge Chromel-Alumel wire at frequent intervals to ensure temperature uniformity, and the windings may be tapped or spaced to reduce the power in hot regions. The thermocouples are insulated by glass and asbestos at points above the ceramic insulation. Swage-lock connectors located 6 in. above the furnace head provide a watertight joint to the tubes leading to the surface of the reactor shielding pool.

The furnace has been tested under water to check the leaktightness and to learn the operating characteristics. At an operating temperature of 350°C the power required was 1500 w, and the hot zone showed temperature uniformity of $\pm 10^\circ\text{C}$ over a length of 4-1/2 in.

The initial experiments planned for execution within the TRIGA reactor have been simplified in order to check the components of the furnace and the experimental procedures during in-reactor operation. In the first set of oxidation experiments, it is proposed to measure the rate of oxidation of copper in the radiation field by means of a multiple-sample technique. Weighed copper foils will be sealed into vitreous silica capsules in pure oxygen at a pressure of 10 mm Hg (as was done in the post-irradiation experiments reported above). Each capsule will be lowered into the reaction furnace via the convoluted aluminum insertion tube. After exposure to the

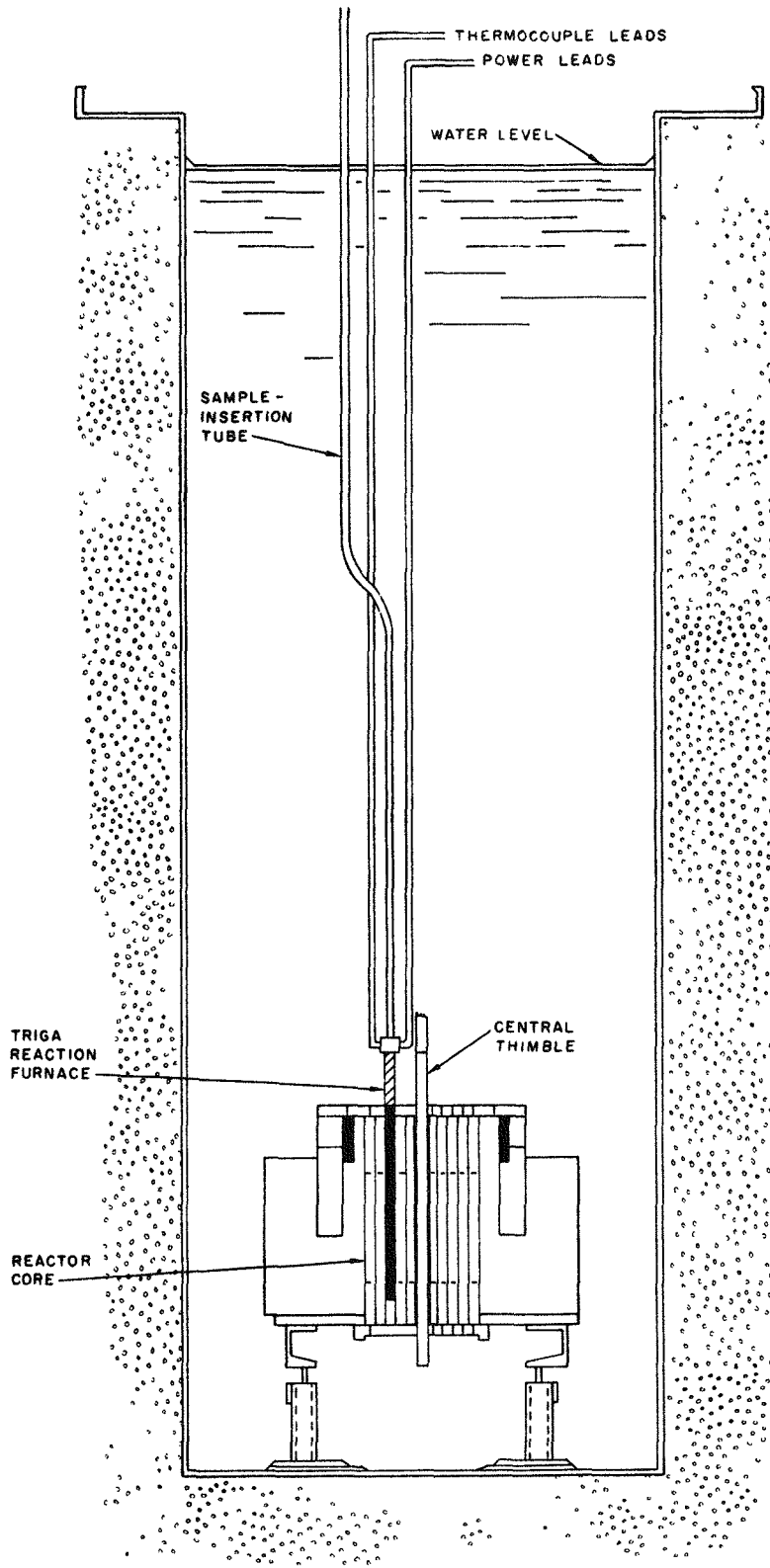


Fig. 11--Location of reaction furnace relative to core in TRIGA reactor

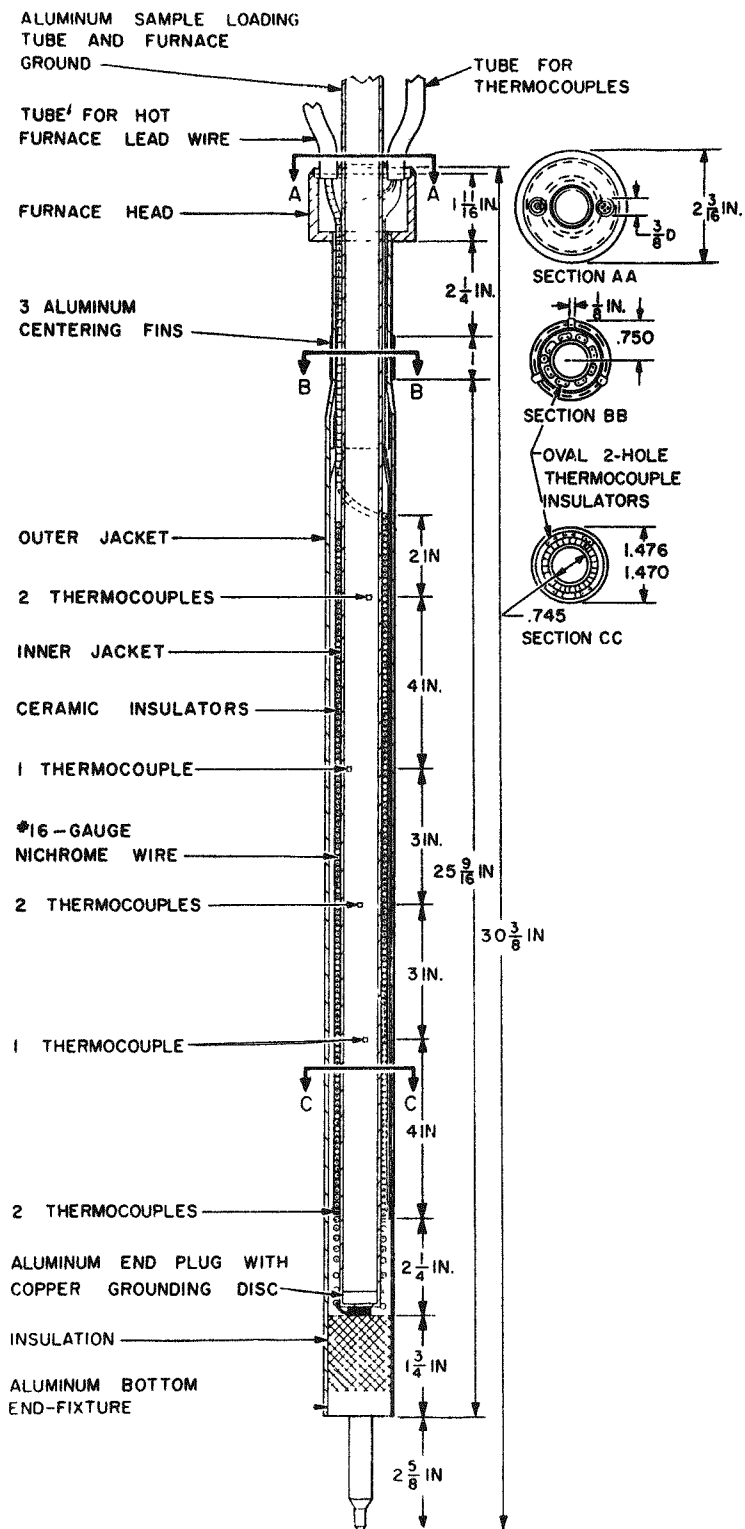


Fig. 12--Furnace for study of reactions of metal or metal oxides with gases in reactor radiation field

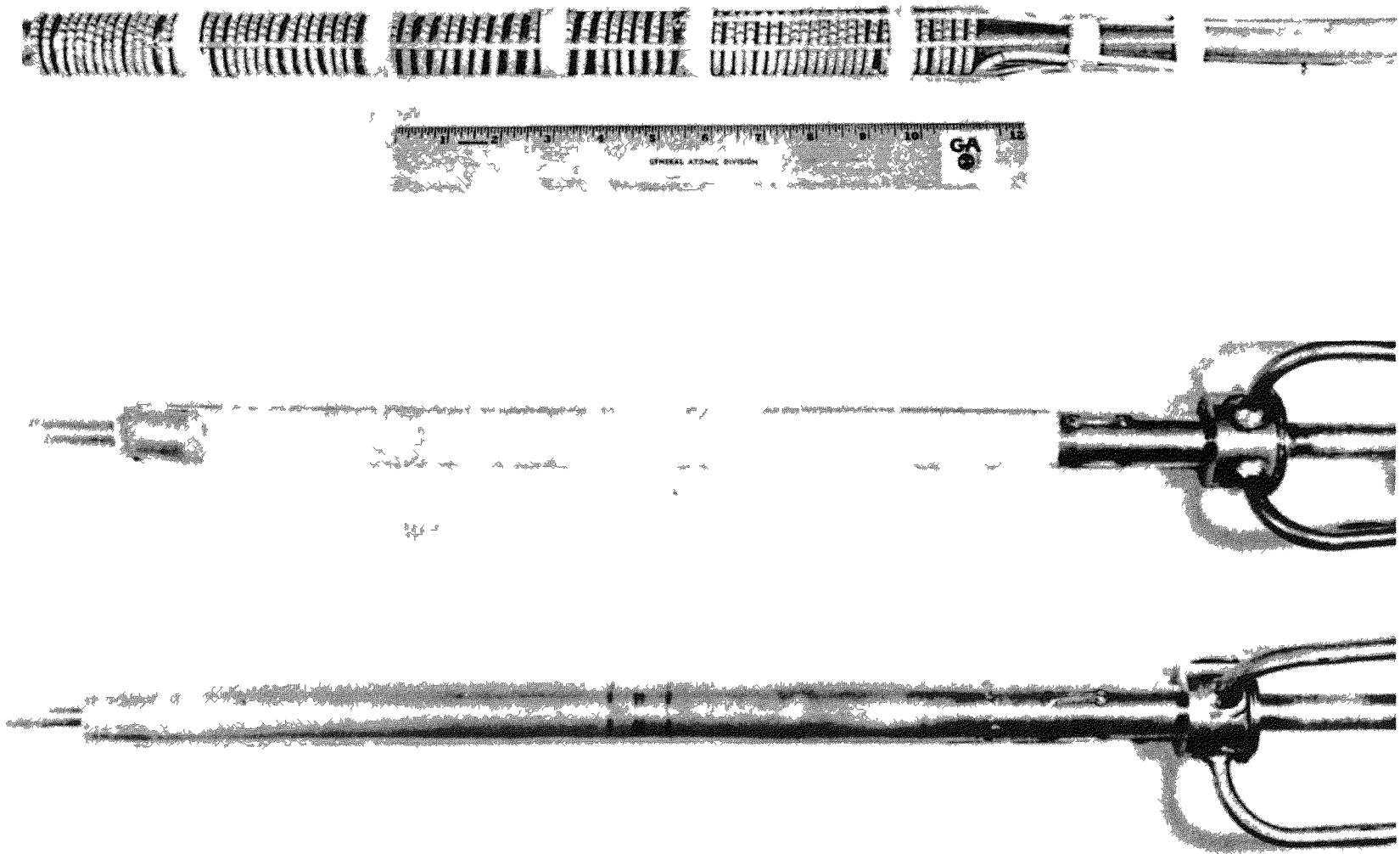


Fig. 13--TRIGA reaction furnace disassembled to display the component parts

radiation field for a given period of time, the capsule will be withdrawn from the furnace and stored to allow the radioactivity to decay to safe levels, and the extent of reaction will be determined by weighing or by optical techniques.

III. REACTIONS WITH AQUEOUS PHASES

The electrochemical mechanisms⁽¹⁷⁾ by which most reactions of metals with aqueous solutions proceed may be illustrated by the simple case of copper in contact with a solution containing cupric ions, which is shown in Fig. 14. Assuming the surface of the undisturbed copper specimen to consist of local anodes and cathodes of potentials E_A and E_C , respectively, the flow of ions from the anodes to the cathodes will follow the polarization curves and will yield an average specimen potential, E_1 , and a corrosion current, i_1 . If the anodes are made more electropositive by irradiation

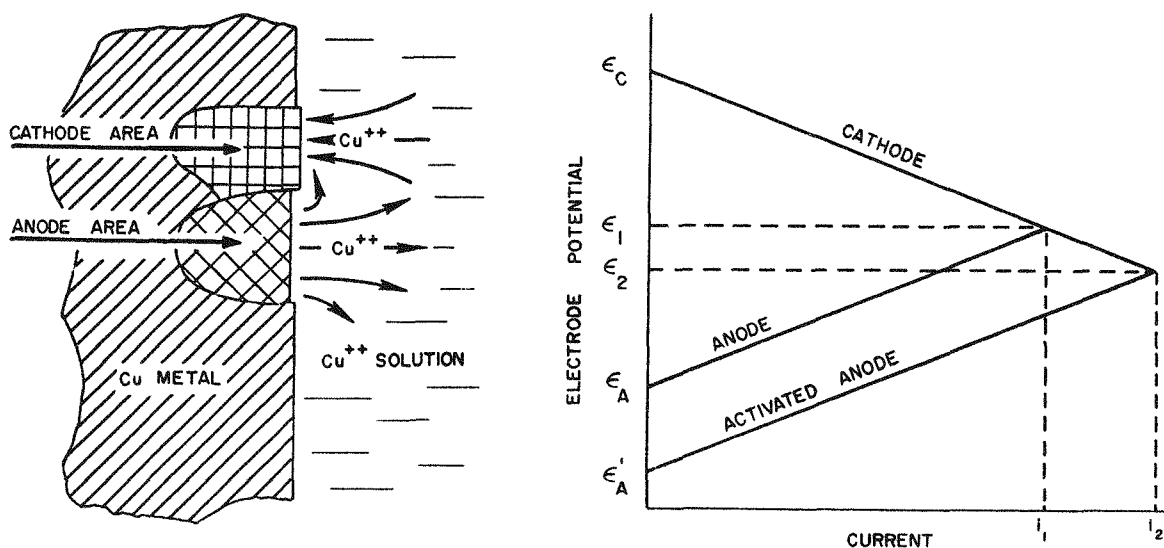


Fig. 14--Schematic diagram illustrating the electrochemical nature of reactions of metals with aqueous solutions; (left) simplified model of copper specimen reacting with aqueous solution of cupric ions, (right) polarization curves for anode, cathode, and activated anode

(e. g., by the precipitation of vacancies and interstitials on a dislocation and thus raising the dislocation line energy), the new anode potential will result in a lower average specimen potential, E_2 , and a larger corrosion current, i_2 . Although the actual values of E_2 and i_2 will depend in a complex manner on a number of variables, such as the chemical nature, polarization curves, and distribution of the local anodes and cathodes, the essential point is that the effects of radiation on a solid taking part in an electrochemical surface reaction with an aqueous solution may be measured in two ways: (1) by measuring the electrode potentials and (2) by measuring the corrosion currents.

ELECTRODE POTENTIALS

Measurements have been made of the electrode potentials of specimens of copper, aluminum, magnesium, and zirconium irradiated in the Brookhaven reactor to a total flux of $nvt = 3.3 \times 10^{19}$ neutrons cm^{-2} . Copper was selected for the initial studies, which involved extensive improvements in the apparatus and technique, since this is the only metal of those listed above which can be expected to form a reversible electrode in equilibrium with an aqueous solution of the metal ions.

The development of the apparatus (see Fig. 15) centered around attaining and maintaining a high degree of cleanliness of the electrodes and the electrolyte. The electrolyte-preparation reservoir or the electrode compartment can be evacuated, and pure argon may be passed through either compartment during transfer of the electrolyte solution or of the electrodes. Greaseless Teflon stopcocks were used at points in contact with the electrolyte, and a stirring device provided a controlled flow of electrolyte over the electrodes. During operation, the apparatus was submerged in a controlled-temperature water bath. The potentials were recorded by means of a Kintel microvolt amplifier coupled to an Esterline-Angus recorder. Four electrodes were employed--two irradiated specimens

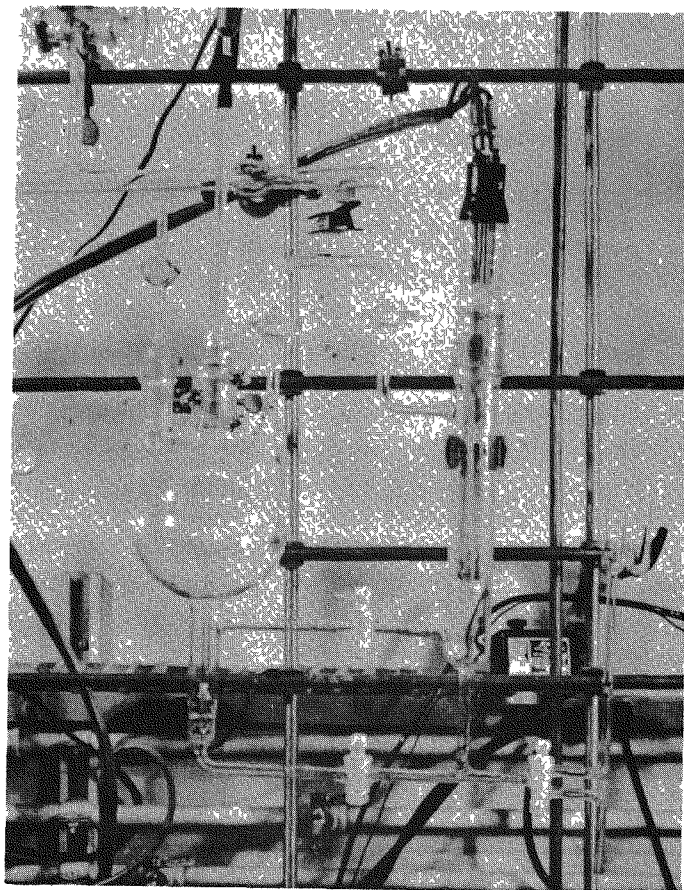


Fig. 15--Apparatus for measurement of electrode potentials of irradiated metal specimens

and two annealed specimens which served as reference electrodes. During the development of the apparatus, cold-worked specimens were used to simulate irradiated specimens and to economize on them.

The electrodes were in the form of 1/8-in. -diameter copper rods which had been annealed at 900°C in vacuum prior to irradiation. The preliminary cleaning of the electrodes was done by bright-dipping them in 50% HNO_3 , rinsing with deaerated distilled water, electropolishing in 50% orthophosphoric acid, rinsing with 0.5% H_3PO_4 , and then rinsing with deaerated distilled water. The final cleaning was done in the electrode compartment, where the rods were electroetched in contact with 0.5 N CuSO_4 prior to a final rinse with the deaerated electrolyte. The electrode

connections and supporting wires were coated with a mixture of 70% beeswax and 30% paraffin.

The electrolyte used with the copper electrodes was 0.5 N CuSO_4 purified by vacuum deaeration in the solution reservoir. The solution was equilibrated with clean copper shot that had been added to the reservoir; darkening of the surface of this copper shot indicated that the purity of the solution had deteriorated.

The electrode potentials of irradiated specimens of copper relative to those of annealed specimens are shown in Fig. 16 as a function of time. The irradiated specimens maintained an anodic potential of about 1 mv for 70 hr, after which the purity of the solution deteriorated. The cold-worked electrodes showed a similar anodic potential of about 1 mv, but this potential began to decay after about 20 hr; these results agree with the measurements of Wernick,⁽¹⁸⁾ who also encountered serious problems of surface contamination during measurements on cold-worked copper.

The effect of temperature on the potentials of the irradiated copper specimens relative to the potentials of the annealed specimens is shown in Fig. 17. There is a definite trend toward a negative temperature coefficient for the potential of the $\text{Cu}(\text{irradiated})/0.5 \text{ N CuSO}_4/\text{Cu}(\text{annealed})$ cell. If the observed electrode potentials can be assumed to be simply related to the reversible potentials of the local anodes, as indicated in the schematic diagram in Fig. 14, the negative temperature coefficient corresponds to a positive entropy of the irradiated copper relative to that of the annealed copper.

The potentials of cells involving the irreversible electrodes of aluminum, magnesium, and zirconium were measured using 1 N KCl solution as the electrolyte. In no case were reproducible or steady potentials observed, and the potential between two annealed specimens was often greater than those between the irradiated and annealed specimens. It was concluded that the cell potentials were dominated by the oxide films formed on the electrode surfaces.

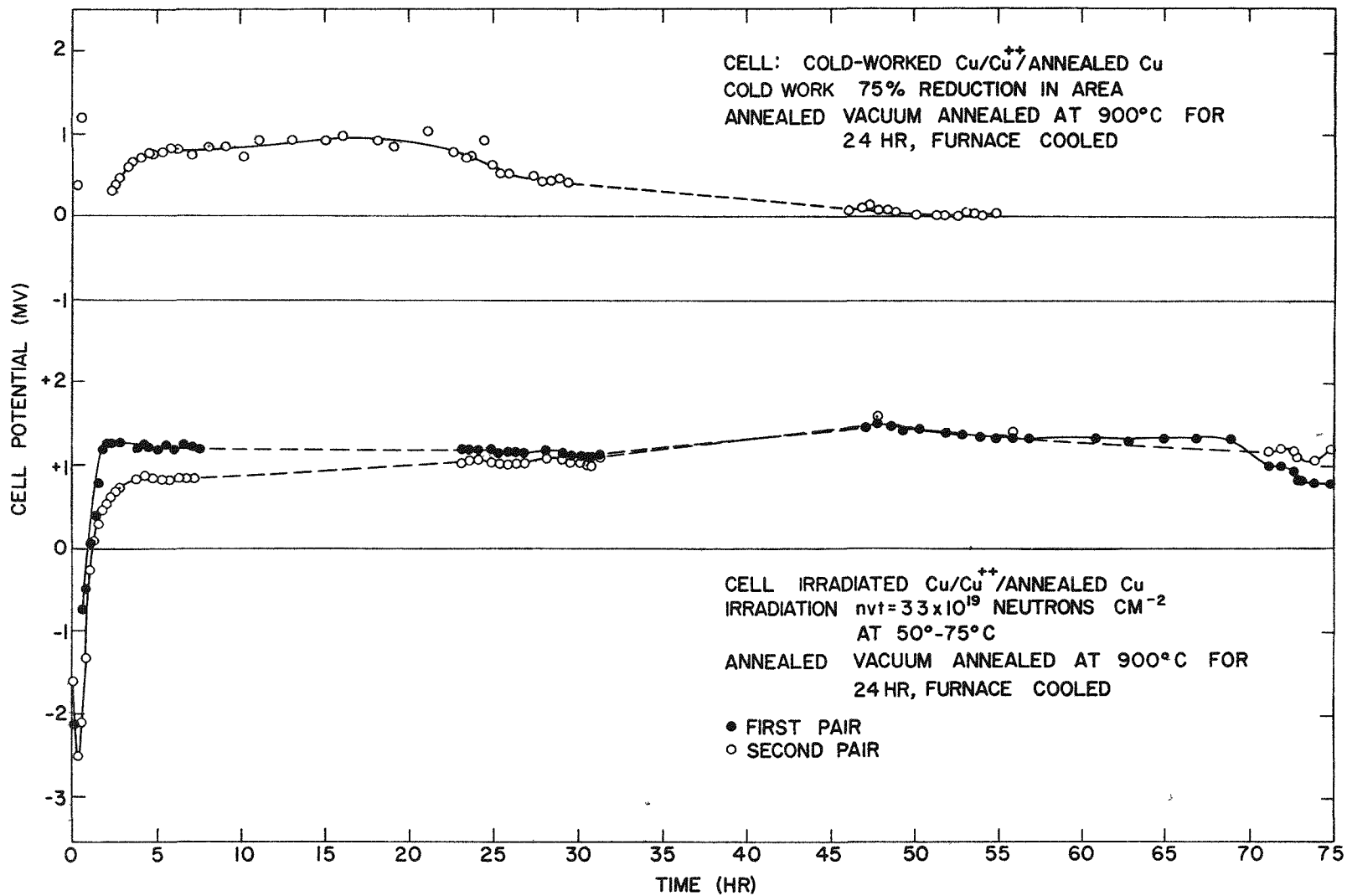


Fig. 16--Electrode potentials of cold-worked and irradiated copper relative to annealed copper

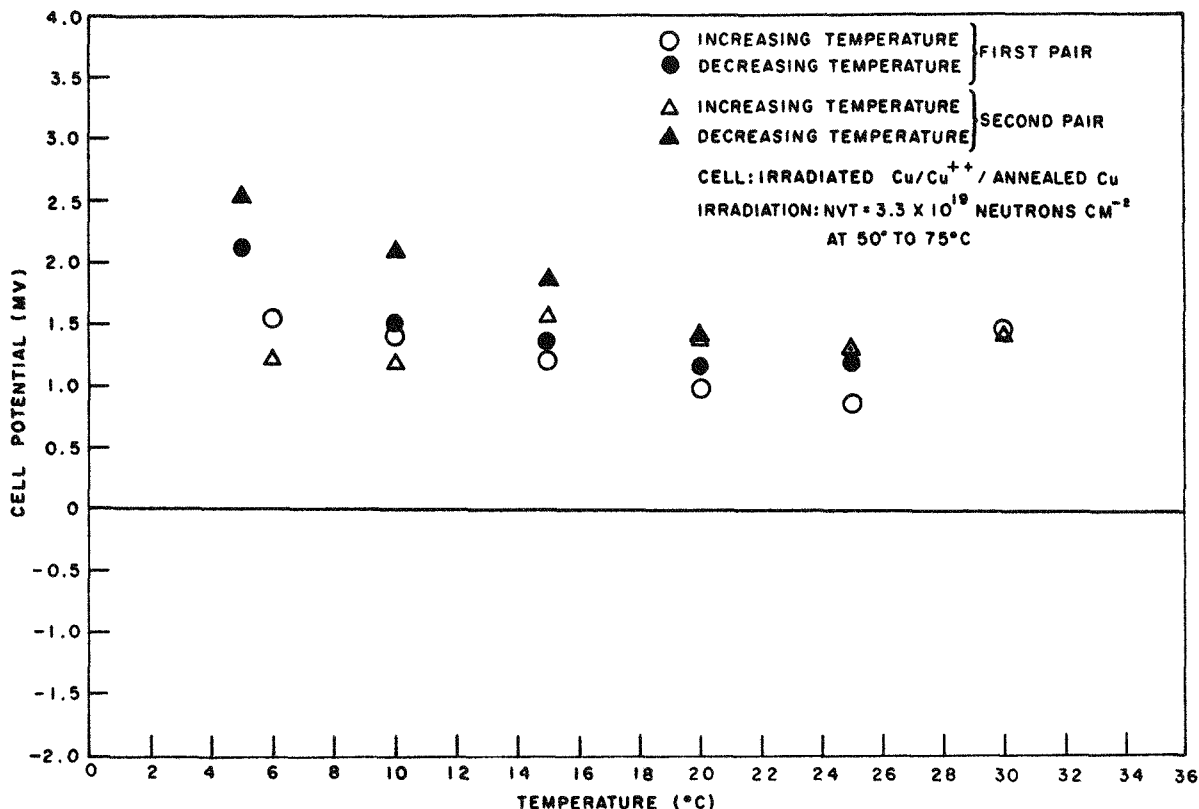


Fig. 17--Effect of temperature on electrode potential of irradiated copper

STUDIES OF DISSOLUTION REACTIONS

In order to measure the corrosion current (designated i_1 and i_2 in Fig. 14) of a specimen in contact with an electrolyte, it is necessary to employ a cathode reaction which is not simply a reversal of the anode reaction. The corrosion current can then be related to the rate of increase of the anode reaction product in the solution. Furthermore, it is desirable to choose a cathode reaction which has a reversible potential only slightly above that of the anode reaction, in order to maximize the relative effect of radiation on the anodic polarization curve.

Copper was selected for these studies for two reasons. First, the results of the electrode-potential measurements reported in the previous section indicate that radiation does affect the local anode reaction potentials, so that the rates of dissolution may be expected to be radiation-sensitive.

Second, the exhaustive studies of the dissolution of copper in ferric solutions recently reported by Ferrari⁽¹⁹⁾ provide an excellent basis for the design of experiments involving irradiated copper specimens. The results obtained by Ferrari show that the dissolution of copper in FeCl_3 solutions is diffusion-controlled at temperatures above 7°C and that the dissolution is influenced by the surface structure at temperatures below 7°C . Thus, the $\text{Fe}^{+++}-\text{Fe}^{++}$ cathode reaction appears to have the sensitivity desired for testing the effects of radiation on the dissolution of copper.

The first set of experiments consisted of direct measurements of the rate of dissolution of annealed, cold-worked, and irradiated specimens of pure copper in $\text{Fe}(\text{NO}_3)_3$ solutions at 5°C . Ferric nitrate was selected because the reaction proceeds more slowly than when FeCl_3 is used and does not have the complications due to chloride ion complexes.

The copper specimens were rolled and cut into two sheets with dimensions of 0.5 by 15 by 25 mm. Two-thirds of the specimens were annealed in vacuum at 900°C for 24 hr, and half of the annealed specimens were subjected to a total radiation of $\text{nvt} = 2.7 \times 10^{18}$ neutrons cm^{-2} in the Brookhaven reactor. The specimens were prepared for irradiation by degreasing, cleaning in 10% HNO_3 , rinsing, and masking to expose exactly 1 cm^2 of surface. The dissolution apparatus is shown in Fig. 18. The reaction flask was filled with 1500 ml of a M/3 $\text{Fe}(\text{NO}_3)_3$ solution which was stirred by a glass propeller at 380 rpm. Aliquot samples of the solution were removed at regular intervals by means of the capillary tube running to the sampling bulb. The Cu^{++} content of each sample was determined by a spectrophotometric method employing Neo-Cuproine (2,9-dimethyl-1,10-phenanthroline hemihydrate) reagent, which is highly specific for copper. The concentration of the copper complex was measured at a wavelength of 457 $\text{m}\mu$.

The results, which are given in terms of the reaction rate constants in Table 1, show that there is no significant difference between the rates of reaction of cold-worked and annealed specimens. However, the average

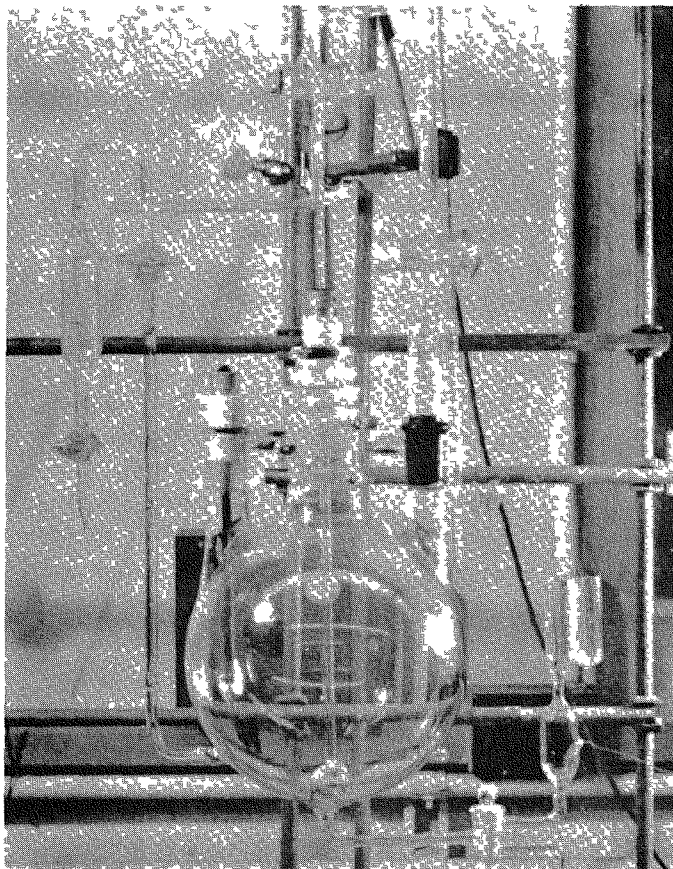


Fig. 18--Apparatus for measurements of rates of dissolution of metals in aqueous solutions

rate of reaction of the irradiated copper specimens is larger than that of the annealed specimens by an amount approximately equal to the estimated uncertainty. Thus, it seems likely that irradiation has enhanced the reactivity of the copper specimens by of the order of 5%.

The next set of experiments was designed to establish optimum conditions for observing the differences in the dissolution rates of irradiated and unirradiated copper specimens. For this purpose four single crystals of copper cut to the (111) face were used. Tragert and Robertson⁽²⁰⁾ have shown that the (111) face is the most stable crystal face for copper. Two crystals were exposed in the TRIGA reactor to a relatively low total radiation of $nvt = 9 \times 10^{16}$ neutrons cm^{-2} . The (111) surfaces were then etched

Table 1
 REACTION-RATE CONSTANTS FOR THE DISSOLUTION OF COPPER
 IN M/3 Fe(NO₃)₃ SOLUTIONS AT 5°C
 (In $\mu\text{g cm}^{-2} \text{sec}^{-1}$)

Annealed Specimens	Cold-worked Specimens	Irradiated Specimens
2.8 ₉ ± 0.8	2.4 ₆ ± 0.7	2.9 ₉ ± 0.4
2.5 ₇ ± 0.5	2.7 ₇ ± 0.2	3.0 ₇ ± 0.2
3.0 ₃ ± 0.2	2.6 ₆ ± 0.2	
2.7 ₇ ± 0.4	2.9 ₇ ± 0.3	
	2.7 ₅ ± 0.2	
Weighted Average		
2.8 ₇ ± 0.2	2.7 ₄ ± 0.2	3.0 ₅ ± 0.2

by the technique developed by Lovell and Wernick⁽²¹⁾ for the development of dislocation etch pits.

An essential feature of a dislocation etchant is that the reactivity of the solution is so closely adjusted to that of the crystal surface that such surface features as dislocation cores are attacked preferentially. In terms of the polarization curves of Fig. 14, such a situation will exist when the cathode reaction potential is less than the "perfect-surface" potential but greater than the potential of the dislocation core. Thus, the use of dislocation etchant solutions in combination with microscopic observations of the etched surfaces offers another means of investigating the enhancement of reactivity of a crystal by irradiation.

The specimens were chemically polished prior to etching in order to obtain smooth initial surfaces. The polishing solution, which was applied at 80°C, was composed of 10 ml HC₂H₃O₂, 10 ml H₃PO₄, 20 ml HNO₃,

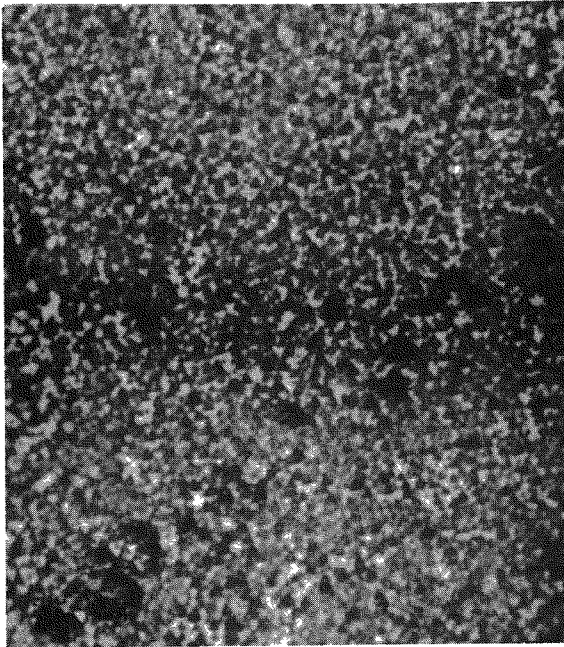
and 0.004 to 0.04 g each of NaNO_3 and NH_4Cl . The dislocation etchant solution was composed of 20 ml saturated aqueous FeCl_3 , 20 ml HCl , 5 ml $\text{HC}_2\text{H}_3\text{O}_2$, and 5 to 10 drops Br_2 . After etching, the specimen was rinsed with NH_4OH to remove Cu_2O films.

The visual observations made with a binocular microscope after various periods of etching showed that the irradiated specimens developed etch pits at a slightly greater rate than did the unirradiated specimens. The two pairs of photomicrographs given in Fig. 19 illustrate this phenomenon. In the upper pair, taken at 1000X after 80 sec of etching, the triangular character of the dislocation etch pits is clearly visible. In the lower pair, taken by the dark-field method at 1000X after 80 sec of etching, the etch pits appear to have fully overlapped to cover the majority of the specimen surface, and the grosser character of the pitting of the irradiated specimens is clearly visible.

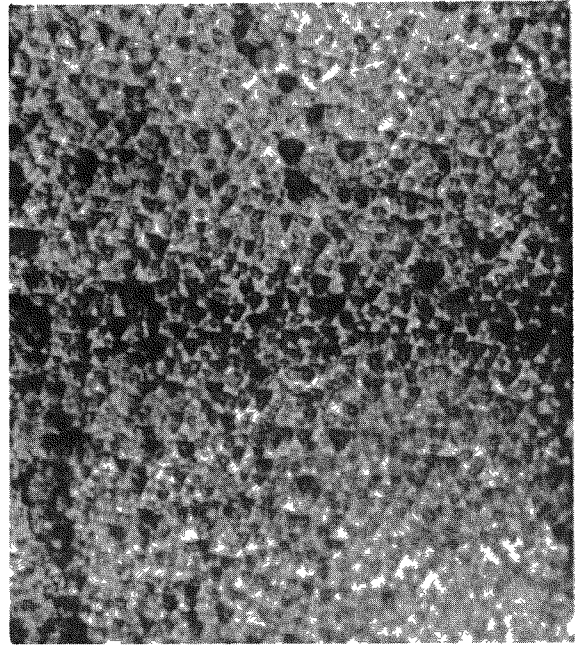
A plausible explanation for the observation that the irradiated crystals develop etch pits more rapidly than the unirradiated crystals is based on the fact that the point defects introduced by irradiation are mobile in copper at room temperature. Consequently, by moving to existing dislocation lines the defects will precipitate on the dislocations and thus raise the line energy and increase the chemical reactivity of the dislocation core at the corroding surface. The following measurements of the hardness of the specimens confirm that radiation-hardening took place at the radiation dose employed:

	<u>Unirradiated Specimens</u>	<u>Irradiated Specimens</u>
Hardness numbers	40.8	44.2
Diamond-pyramid hardness scale	41.8	45.0

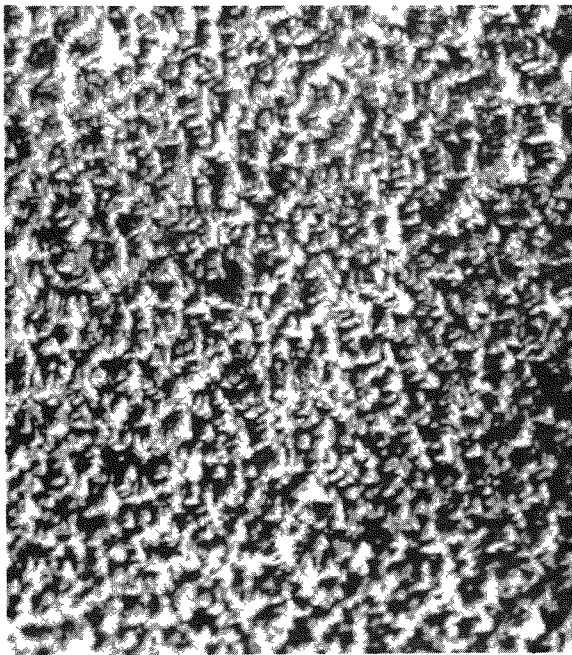
The next step in the investigation of dissolution processes involved the use of the electropolishing microscope shown in Fig. 20 to observe the surface of the specimen during the dissolution process. The aim of this work was to obtain further evidence for the existence of local radiation-



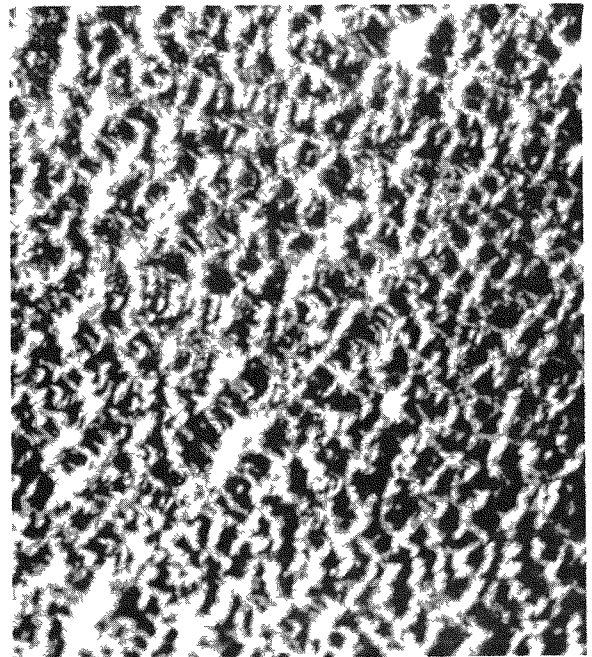
Annealed copper



Irradiated copper



Annealed copper



Irradiated copper

Fig. 19--Etch-pit patterns produced on (111) face of single crystals of copper after 80 sec of etching with an etchant developed for preferential etching of dislocation core; (top) bright-field illumination, (bottom) dark-field illumination; 1000X

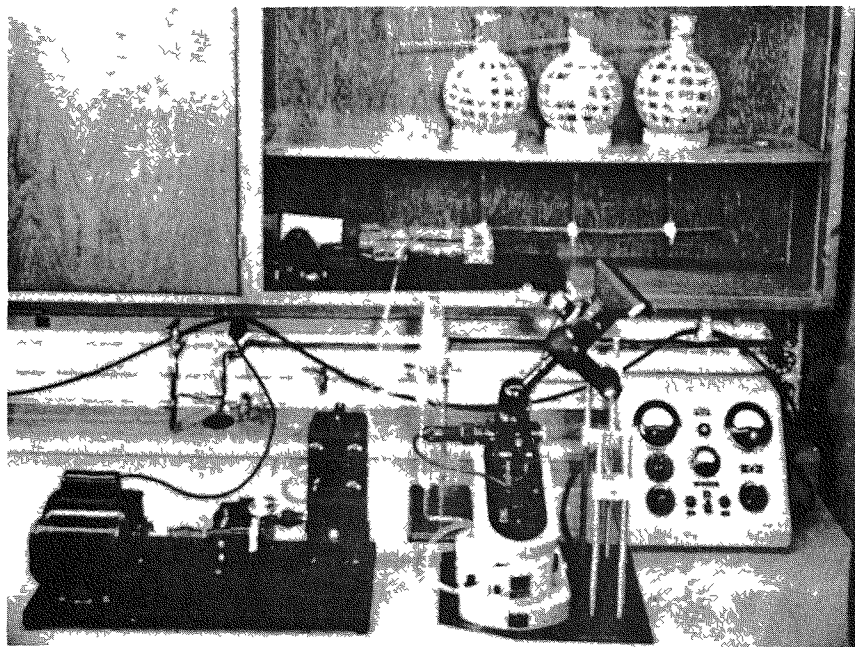
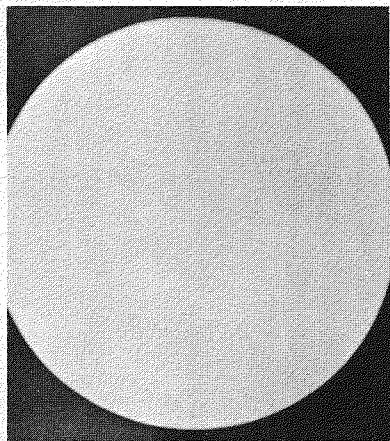


Fig. 20-- Zeiss electropolishing microscope used for direct observations of specimen surface during dissolution; circulating pump and solution manifold are also shown

activated anode areas.

By using the Zeiss electropolishing microscope (at 210X), the surface of a specimen can be directly observed while a solution is pumped over the specimen at a controlled rate. An electropolishing potential may be applied to the specimen if desired. The initial studies were made using polycrystalline copper specimens and solutions of $\text{Fe}(\text{NO}_3)_3$ and FeCl_3 . The copper specimens were annealed in vacuum at 900°C , and half of the specimens were subjected to an irradiation of $nvt = 2.7 \times 10^{18}$ neutrons cm^{-2} in the Brookhaven reactor.

A series of comparison photographs of annealed and irradiated specimens reacted with $M/4 \text{FeCl}_3$ at $25^\circ \pm 2^\circ\text{C}$ is given in Fig. 21. Owing to difficulties in attaining equal flow rates in each case, the differences in appearance cannot be definitely attributed to radiation effects. The solution



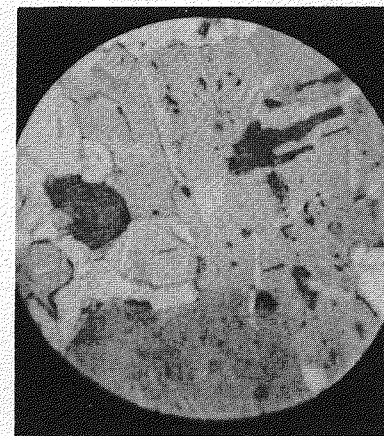
0 sec



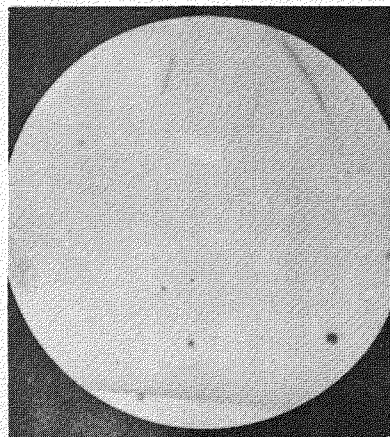
50 sec



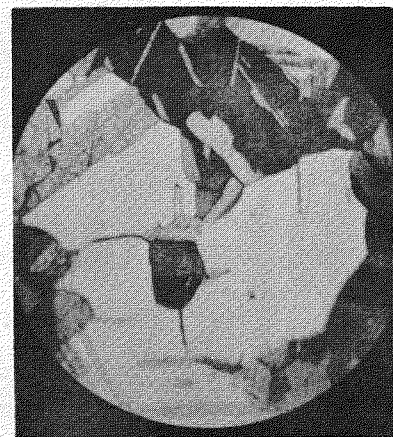
100 sec



200 sec



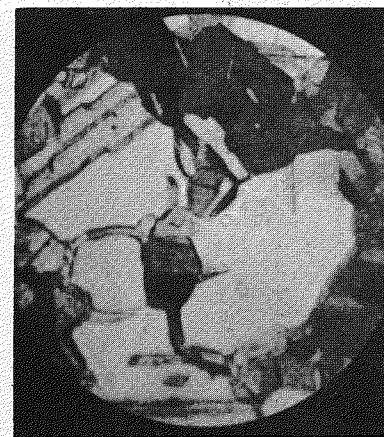
0 sec



50 sec



100 sec



200 sec

Fig. 21--Surfaces of copper specimens during dissolution in M/4 FeCl_3 at $25 \pm 2^\circ\text{C}$;
(top) irradiated copper, (bottom) annealed copper (etching time is
shown beneath each photomicrograph); 210X

manifold system shown in Fig. 20 has recently been set up, and, by means of a constant-head gravity-flow system, equal flow rates should be achievable for further investigations. Another purpose of the solution manifold is to permit chemical cleaning of the specimens followed by the dissolution process without an intervening exposure to air.

IV. ACKNOWLEDGMENTS

Invaluable assistance and direction during the design and construction of the TRIGA reactor furnace facility has been provided by J. M. Tabin. J. C. Bokros and G. R. Schmitt, Jr., have assisted and advised in the studies of dislocation etch pits, and the extensive discussions with R. H. Chambers have been a valuable aid in this research. The electronic control and recording system for the automatic recording microbalance was designed and constructed by H. Schick of the Electronics Group.

Appendix
METHODS OF IRRADIATION

The methods of specimen preparation and irradiation were discussed in the previous summary report (see Ref. 1). In view of the mobility of the point defects produced in metals during irradiation,⁽²²⁾ it was felt desirable to establish some simple monitoring technique to provide an independent measure of the extent of radiation effects retained in the materials after the thermal treatment involved in the surface-reaction experiments. In the earlier work, measurements of hardness served this purpose; however, hardness measurements are to some extent destructive in the sense that the dislocation and grain structures of the specimens are disturbed.

The electrical resistivity of metals is highly sensitive to crystal defects produced by radiation,⁽²²⁾ and measurements of this property can be made conveniently and nondestructively. The irradiations currently in progress have therefore included coiled wire monitors prepared from the same material as the specimens. The coils are wound on alumina cores, as shown in Fig. 22, and tabs are provided for attaching electrical leads without disturbing the coil proper. The resistances are of the order of 1 ohm, and the measurements are made on a Wheatstone bridge of high sensitivity.

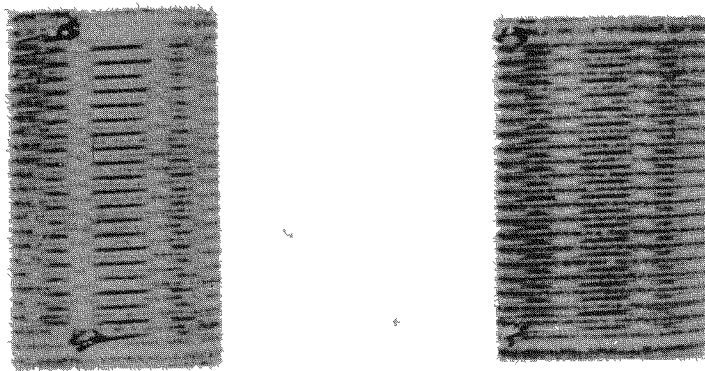


Fig. 22--Resistance monitors for irradiation experiments; (left) iron, (right) nickel

REFERENCES

1. Irradiation Effects on the Surface Reactions of Metals. Summary Report, General Atomic Report GACP-563, October 31, 1958.
2. Simnad, M. T., "Influence of Radiation Upon Corrosion and Surface Reactions of Metals and Alloys," in J. J. Harwood, H. H. Hausner, J. G. Morse, and W. G. Ranch (eds.), Effects of Radiation on Materials, Reinhold Publishing Corp., New York, 1958, pp. 126-143.
3. Technical Foundations of TRIGA, General Atomic Report GA-471, August 27, 1958; Torrey Pines TRIGA Reactor, General Atomic Report GA-691, March 10, 1959.
4. Kubaschewski, O., and B. E. Hopkins, Oxidation of Metals and Alloys, Butterworths, London, 1953.
5. Tylecote, R. F., "Review of Published Information on the Oxidation and Scaling of Copper and Copper-Base Alloys," J. Inst. Metals, Vol. 78, 1950, p. 259.
6. Lustman, B., and R. F. Mehl, "Low-temperature Oxidation of Single Crystals of Copper," Trans. AIME, Vol. 143, 1941, p. 246.
7. Young, F. W., Jr., J. V. Cathcart, and A. T. Gwathmey, "The Rates of Oxidation of Several Faces of a Single Crystal of Copper as Determined with Elliptically Polarized Light," Acta Met., Vol. 4, 1956, p. 145.
8. Harris, W. W., F. L. Ball, and A. T. Gwathmey, "The Structure of Oxide Films Formed on Smooth Faces of a Single Crystal of Copper," Acta Met., Vol. 5, 1957, p. 574.
9. Gwathmey, A. T., and K. R. Lawless, "The Influence of Crystal Orientation on the Oxidation of Metals," to be published.
10. Holmes, D. K., J. W. Corbett, R. M. Walker, J. S. Koehler, and F. Seitz, "On the Interpretation of Radiation Effects in the Noble Metals," in Proceedings of the Second United Nations International Conference on the Peaceful Uses of Atomic Energy, Vol. 6, United Nations, Geneva, 1958, p. 274.
11. Young, F. W., Jr., On the Effect of Reactor Exposure on the Rate of Oxidation of Copper Single Crystals, Oak Ridge National Laboratory Report CF-55-3-70, March 9, 1955.
12. Rhodin, T. N., Jr., "Surface Studies with the Vacuum Microbalance: Instrumentation and Low-Temperature Applications," Advances in Catalysis, Vol. 5, 1953, p. 39.

13. Gulbransen, E. A., "Surface Studies with the Vacuum Microbalance: High Temperature Reactions," Advances in Catalysis, Vol. 5, 1953, p. 119.
14. Jennings, T. J., "Microbalance Techniques," in T. J. Gray, et al., The Defect Solid State, Chapter 7, "Experimental Techniques," Interscience Publishers, New York, 1957.
15. Cochran, C. N., "Automatic Recording Vacuum Microbalance," Rev. Sci. Instr., Vol. 29, 1958, p. 1135.
16. Czanderna, A. W., and J. M. Honig, "Sensitive Quartz Beam Microbalance," Anal. Chem., Vol. 29, 1957, p. 1206.
17. Yang, L., and M. T. Simnad, "Effect of Stress and Deformation on Electrode Potential, Polarization, and Rate of Corrosion," to be published.
18. Wernick, J. H., A Study of the Effect of Plastic Deformation on the Electrochemical Behavior of Copper, Ph.D. dissertation, Pennsylvania State University, 1954.
19. Ferrari, H. M., The Kinetics and Mechanism of Dissolution of Copper in Ferric Chloride Solutions, Ph.D. dissertation, University of Michigan, 1958.
20. Tragert, W. E., and W. D. Robertson, "The Crystallographic Dependence of the Oxidation Potential of Solid Copper," J. Electrochem. Soc., Vol. 102, 1955, p. 86.
21. Lovell, L. C., and J. H. Wernick, "Dislocation Etch Pits and Polygonization in High-Purity Copper," J. Appl. Phys., Vol. 30, 1959, p. 590.
22. Dienes, G. J., and G. H. Vineyard, Radiation Effects in Solids, Interscience Publishers, New York, 1958.